

# Mechanical Properties of Additively Manufactured Titanium Alloy Sandwich Structures for Thermal Protection

Philipp Nieke<sup>1†</sup>, Vladimir Yotov<sup>2</sup>, Guglielmo S. Aglietti<sup>2</sup>, Nicholas J. Rattenbury<sup>3</sup>, John E. Cater<sup>4</sup>

<sup>1</sup>The University of Auckland, Department of Engineering Science, Auckland, New Zealand

<sup>2</sup>The University of Auckland, Space Institute - Te Pūnaha Ātea, Auckland, New Zealand

<sup>3</sup>The University of Auckland, Department of Physics, Auckland, New Zealand

<sup>4</sup>University of Canterbury, Department of Mechanical Engineering, Christchurch, New Zealand

p.nieke@auckland.ac.nz

<sup>†</sup>Corresponding author

## Abstract

In recent years, sandwich structures with lightweight lattice cores have been considered for active and passive thermal protection systems (TPSs) for aerospace applications.<sup>5,6,9,14,22</sup> Metal additive manufacturing provides a relatively fast method of physically realising such complex structures with the advantage of a low and controllable core density.<sup>4,18</sup> While most studies determine the heat transfer characteristics of those TPSs, the performance under dynamic mechanical loads such as vibration has not yet been studied extensively.<sup>14</sup> Thus, this contribution focuses on vibration testing and correlation with numerical modal analysis of six cylindrical sandwich samples with open-cell lattice cores. The lattice cores are based on a body-centred cubic (BCC) unit cell with an edge length of 5 mm. To study the influence of the lattice properties, three relative core densities (resulting from nominal strut diameters of 0.5 mm, 0.8 mm, and 1.0 mm), and two lattice thicknesses (15 mm and 25 mm) were manufactured using Electron Beam Melting in Grade 5 Titanium (Ti-6Al-4V). Low-level random vibration tests were performed within a frequency range from 20 Hz to 2000 Hz on a 1D shaker in the axial and lateral directions successively. A 586.5 g dummy mass was mounted on top of the samples, such that the assembly would have natural frequencies (NFs) lower than the maximum excitation frequency. Two pairs of orthogonal bending modes, an axial mode and a torsion mode, were identified in the specified frequency range. The natural frequency of the bending mode was successfully measured for all samples. For the axial mode, the exact NFs could only be determined for three of the samples, as the remainder were above 2 kHz. Depending on the lattice parameters, the NFs ranged from 180 Hz to 804 Hz and from 752 Hz to 1468 Hz, respectively. The equivalent Young's moduli of the homogenised lattice cores were calculated under the assumption of an undamped single-degree-of-freedom (SDOF) spring-mass system. The derived values were lower than analytical predictions for metal foams<sup>12</sup> and BCC lattices.<sup>23</sup>

## 1. Introduction

Thermal Protection Systems (TPSs) are required to safely return payloads from space to Earth.<sup>8</sup> However, it has been recognised that conventional TPS manufacturing is labour-intensive and typically results in long lead times, quality issues, and high costs.<sup>3</sup> Furthermore, the number of flight-qualified TPS alternatives is relatively small.<sup>3</sup> Recently, NASA investigated additively manufactured thermal protection systems (AMTPSs).<sup>19</sup> Additive manufacturing (AM) offers fast development times, improved quality and potentially lower costs due to automated operation (under the presumptions of maintained TPS performance).<sup>19</sup>

NASA's activities accumulated in a dedicated AMTPS workshop that identified potential uses in four general TPS applications: launch vehicles and landers, vehicles entering from low earth orbit, hypersonic vehicles and vehicles for planetary missions. Key findings included that low costs and short lead times were important TPS metrics, and that current TPS materials were difficult to procure. Hence, a broader spectrum of TPS solutions was desired that includes ablative, reusable, and hot structures. The potential of AM to achieve these developments was noted.<sup>19</sup>

Further studies, specifically in metallic AMTPS, have been published.<sup>15,22</sup> Lin et al.<sup>15</sup> investigated integrated TPSs inspired by the cellular structure of the Norway spruce stem. Heat transfer simulations and hot disk experiments were carried out for temperatures up to 300 °C. The samples were produced from Ti-6Al-4V powder by Selective Laser

## MECHANICAL PROPERTIES OF TITANIUM ALLOY SANDWICH STRUCTURES

Melting (SLM). Xu et al.<sup>22</sup> compared three integrated TPSs based on lattice structures. Two of them incorporated structures manufactured of Ti-6Al-4V by SLM. Thermal and structural analyses were performed using FEA, and blow lamp experiments up to 800 °C were conducted. Dynamic mechanical testing under vibration loads was not the focus of these studies.

Le et al.<sup>14</sup> reviewed advanced sandwich structures for TPSs in hypersonic vehicles. The authors showed that sandwich structures may be used for passive, semi-passive and active thermal management concepts. Various sandwich core designs were discussed, including honeycomb cores, corrugated cores, lattice cores and others. The lower relative density and higher specific strength of lattice cores were highlighted compared to honeycomb and corrugated cores. However, the authors pointed out a need for more knowledge of the behaviour of additively manufactured sandwich structures under vibration loads.

Vibration tests are an integral part to qualify space hardware<sup>7</sup> and can be non-destructive when carried out at low levels. The present work focuses on low-level random vibration testing of sandwich structures with lattice cores.

## 2. Materials and Methods

### 2.1 Additive Manufacturing

Initially, cylindrical sandwich samples were prepared for plasma wind tunnel testing at the arc-heated facility L2K at the German Aerospace Center.<sup>17</sup> In an attempt to make the most of the test articles manufactured, 6 unused back-up samples were prepared for mechanical testing. The cylindrical design with a diameter of approximately 50 mm was selected to satisfy the requirements of the L2K facility. Each sample consisted of a lattice core between a solid front and a back sheet. The core comprised a volume lattice and a surface lattice to cover the curved lateral surface. Both lattices were based on a body-centred cubic (BCC) unit cell constructed of struts with a cell edge length of 5 mm. A gradual change of cross-sections between the lattice core and the solid face sheets was ensured by a transition layer consisting of fillets with a radius of 2 mm. Two different sample thicknesses and three lattice core densities were obtained by varying the lattice height and the lattice strut diameter. The nominal strut diameters of 0.5 mm, 0.8 mm and 1.0 mm resulted in the relative nominal lattice densities of approximately 5 %, 12 % and 18 %.

The samples were produced in Ti-6Al-4V alloy via EBM (GE Arcam EBM Q10) by a commercial additive manufacturing provider. After printing, the top faces were turned on a lathe to achieve a smooth surface finish. Six holes were drilled and tapped on each side of the cylinders to connect the samples with an interface plate of the shaker and a steel dummy mass. The steel dummy, including six fasteners, had a mass of 586.5 g. Finite element analysis (FEA) was used to estimate the NFs and size the dummy mass. Note that the samples contained six radial holes parallel to the solid faces to accommodate thermocouple sensors, and three additional mounting holes in the back face that were initially intended to connect the samples to a sample holder in the L2K facility and were not used in the current study.

Figure 1 displays the manufactured samples after printing, machining, drilling and tapping, with their front faces upwards, showing the M3 threads used to connect the dummy mass. Table 1 shows the geometric parameters, the relative lattice density and the mass of the samples.

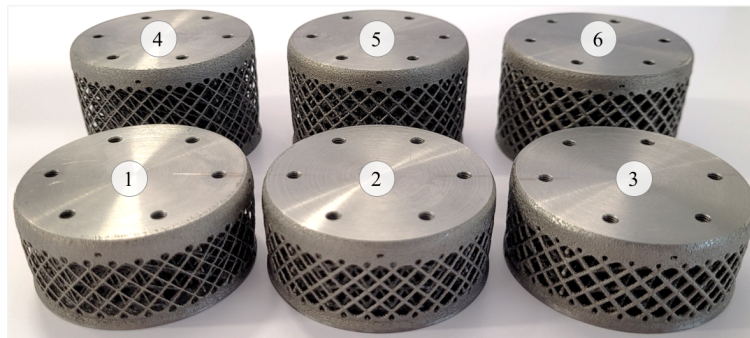


Figure 1: Manufactured samples after printing, turning, drilling and tapping. The short samples are positioned in the front row, and the tall samples are in the back row. Lattice densities increase from left to right. The number labels correspond to the sample numbers listed in Table 1.

Solid tensile specimens were additively manufactured in the same build as the samples and the tensile test result was provided by the manufacturer. The ultimate tensile strength (UTS), the yield strength, the elongation and the reduction of area were all above the minimum requirements of ASTM F2924 (see Table 2), which ensures appropriate material quality.

## MECHANICAL PROPERTIES OF TITANIUM ALLOY SANDWICH STRUCTURES

Table 1: Printed Samples after Turning, Drilling and Tapping

#	Sample	Thickness* mm	Strut Diameter + mm	Relative Lattice Density+ %	Mass* g
1	Short Sample, Light Lattice	21.6	0.5	5.0	65.7
2	Short Sample, Medium Lattice	21.6	0.8	12.1	75.8
3	Short Sample, Heavy Lattice	20.3	1.0	18.1	81.9
4	Tall Sample, Light Lattice	31.4	0.5	5.0	71.7
5	Tall Sample, Medium Lattice	31.4	0.8	12.2	84.0
6	Tall Sample, Heavy Lattice	31.0	1.0	18.2	94.7

\* Measured, + Nominal, # Calculated

Table 2: Solid Ti-6Al-4V Tensile Test Result Provided by Manufacturer, and Minimum Requirements of ASTM F2924

	UTS MPa	Yield (0.2 % Offset) MPa	Elongation %	Reduction of Area %
Tested Sample	1017	938	20	46.7
Min. Requirements	895	825	10	15

## 2.2 Finite Element Analysis

Modal analysis simulations were performed for all six samples using FEA (nTopology version 3.37.3). The dummy mass was modelled as a steel cylinder with a 50 mm diameter and a 40 mm height. The cylinder was seamlessly joined to the top of the sample. A fixed boundary condition (no displacement) was applied to the bottom face of the sample. Mesh convergence was initially studied using Sample 4 (Tall Sample, Light Lattice). The results of the mesh convergence study are shown in Table 3. Doubling the number of elements (Mesh 2 to Mesh 5) changed peak frequencies by < 1 % for both the bending mode and the axial mode. This was considered sufficiently resolved, and the settings used to generate Mesh 2 were also used to mesh the other samples. Table 4 shows the number of solid elements in the meshes used for the individual test cases. Second order elements were used throughout.

Table 3: Mesh Convergence Study using Sample 4

Mesh	Number of Elements	Bending Mode	Axial Mode
		$f_{Peak}$ , Hz	$f_{Peak}$ , Hz
1	510,200	210.9	849.3
2	582,944	210.1	847.2
3	690,598	209.3	844.6
4	924,691	209.7	845.3
5	1,182,999	209.4	844.3
6	1,400,174	209.1	843.4

Table 4: Mesh Overview for Modal Analyses

#	Sample	Volume Elements
1	Short Sample, Light Lattice	416,978
2	Short Sample, Medium Lattice	634,932
3	Short Sample, Heavy Lattice	815,856
4	Tall Sample, Light Lattice	582,944
5	Tall Sample, Medium Lattice	963,888
6	Tall Sample, Heavy Lattice	1,225,261

## MECHANICAL PROPERTIES OF TITANIUM ALLOY SANDWICH STRUCTURES

**2.3 Vibration Tests**

Low-level random vibration tests were performed on a 1D shaker (Dongling ES-20-320) in the axial and lateral directions successively. The frequency ranged from 20 Hz to 2000 Hz, and the root mean square (rms) of the vibration loads was 0.5  $g_{rms}$  and 1.0  $g_{rms}$  in both directions. The loading time was 2 min, respectively.

For each test, the sample was mounted between the interface plate and the dummy mass. A torque wrench set to 2 N m was used to fasten the bolts reproducibly. The acceleration response was measured using a 10 mV/g triaxial accelerometer glued to the top of the dummy mass. Figure 2 shows an annotated photograph of the test assembly mounted on the shaker slip table.

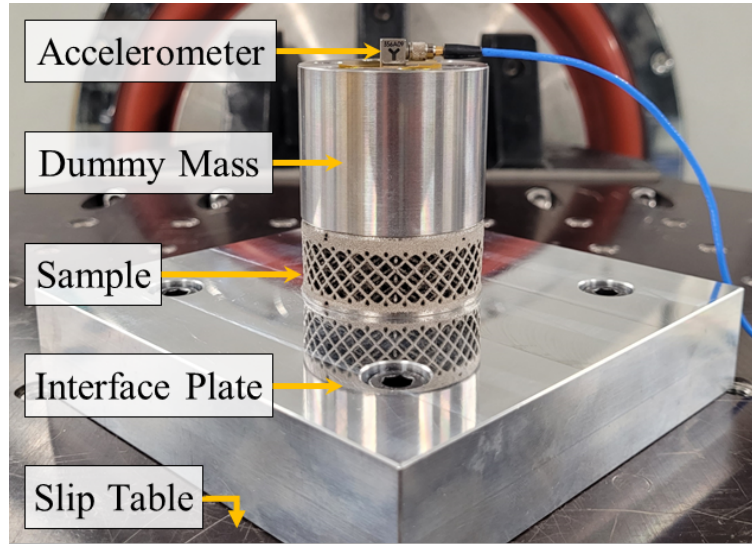


Figure 2: Test assembly mounted to the shaker slip table.

In order to compute the equivalent Young's moduli of the tested samples from the measured NFs, the lattice core sandwich with dummy mass combinations were approximated by undamped SDOF systems (note that this neglects the mass of the lattice samples and any shear effects). A cantilever beam system was used for the lateral load case and a spring-mass system for the axial load case. For a cantilever beam system (loaded at the free end), the Young's modulus is

$$E = 4\pi^2 f^2 m \frac{l^3}{3I}, \quad (1)$$

with the mass  $m$ , frequency  $f$ , length  $l$  and second area moment  $I$ .<sup>21</sup> The second moment of area  $I$  of a circular cross-section is

$$I = \frac{\pi d^4}{64}, \quad (2)$$

where  $d$  is the sample diameter.

The Young's modulus for a spring-mass system is

$$E = 4\pi^2 f^2 m \frac{l}{A}, \quad (3)$$

with the cross-sectional area  $A$  (assuming a homogenised circular cross-section).<sup>21</sup>

**2.4 Analytical Models**

The general mechanical behaviour of frames, foams<sup>1</sup> and lattice structures can be described by the Maxwell stability criterion<sup>16</sup> (in three dimensions):

$$M = s - 3n + 6, \quad (4)$$

with the number of struts  $s$  and the number of nodes  $n$ . The Maxwell number  $M$  determines the expected mechanical response of a lattice.  $M < 0$  indicates an under-stiff lattice with bending-dominated behaviour, whereas  $M \geq 0$  indicates a stiff or an over-stiff lattice structure with stretch-dominated behaviour.

## MECHANICAL PROPERTIES OF TITANIUM ALLOY SANDWICH STRUCTURES

The Maxwell number  $M$  of the BCC lattice studied in this paper is  $-13$  as the BCC unit cell has nine nodes ( $n = 9$ ) and eight struts ( $s = 8$ ). Therefore a bending-dominated behaviour is expected, with high compliance and relatively low strength. The high compliance is expected to be advantageous for a TPS application that involves high thermal gradients and has only secondary absolute strength requirements. Another advantage of BCC lattices is their low relative density that results in associated mass savings.<sup>14</sup>

Ashby et al.<sup>2</sup> noted that the Young's modulus of metal foam is best determined through dynamic testing. Gibson and Ashby<sup>12</sup> presented an analytical relationship for the Young's modulus of a bending-dominated structure (open-cell foam) as a function of its relative density  $\rho_{\text{relative}} = \rho_{\text{foam}}/\rho_{\text{solid}}$ :

$$E_{\text{foam}} = \rho_{\text{relative}}^2 E_{\text{solid}}. \quad (5)$$

Zhang et al.<sup>23</sup> conducted vibration tests of additively manufactured sandwich panels with lattice cores. These panels were part of a generic satellite structure and made of the aluminium alloy AlSi10Mg. This work determined the Young's modulus of a BCC cell lattice specifically:

$$E_{\text{bcc}} = \frac{\sqrt{3}\pi}{9} \left( \frac{d_{\text{strut}}}{d_{\text{cell}}} \right)^2 E_{\text{solid}}, \quad (6)$$

with the strut diameter  $d_{\text{strut}}$ , and the cell size  $d_{\text{cell}}$ .

Both expressions require the Young's modulus of the solid material, which is typically  $E_{\text{solid}} \approx 110$  GPa for the Ti-6Al-4V alloy.<sup>20</sup>

### 3. Results and Discussion

Figure 3 illustrates the shapes of the bending and axial modes. The modal analysis predicted an additional torsional mode in the frequency range up to 2000 Hz. However, as expected, it is not excited with the tests performed, and would otherwise still not be detectable due to the accelerometer placement in the center of the sample.

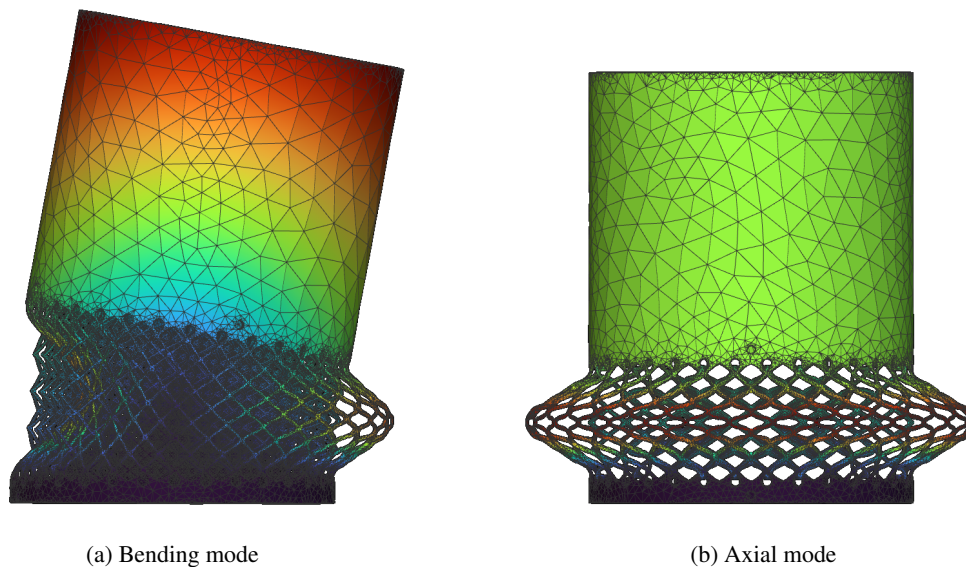


Figure 3: Illustration of relevant mode shapes using the modal analysis results for Sample 4. The colour indicates the displacement of individual elements, where red is large and blue is small.

Figure 4 shows the frequency response functions (FRFs) under the lateral load of  $0.5 \text{ g}_{\text{rms}}$  of (a) the short samples and (b) the tall samples. In both cases, the peak frequencies increase with the lattice density. Additionally, short samples show higher peak frequencies than corresponding tall samples. The peak frequencies of the FRFs of the  $1.0 \text{ g}_{\text{rms}}$  tests were identical, which indicated that no damage (such as plastic deformation or breaking of struts) occurred during the first set of tests at  $0.5 \text{ g}_{\text{rms}}$ .

Similar trends are visible in Figure 5 for the samples under the vertical load of  $0.5 \text{ g}_{\text{rms}}$ . This load direction excites the axial mode with higher peak frequencies. In the cases of Sample 2, Sample 3, and Sample 6, peak frequencies were above the limit of 2000 Hz and, therefore, not captured.

## MECHANICAL PROPERTIES OF TITANIUM ALLOY SANDWICH STRUCTURES

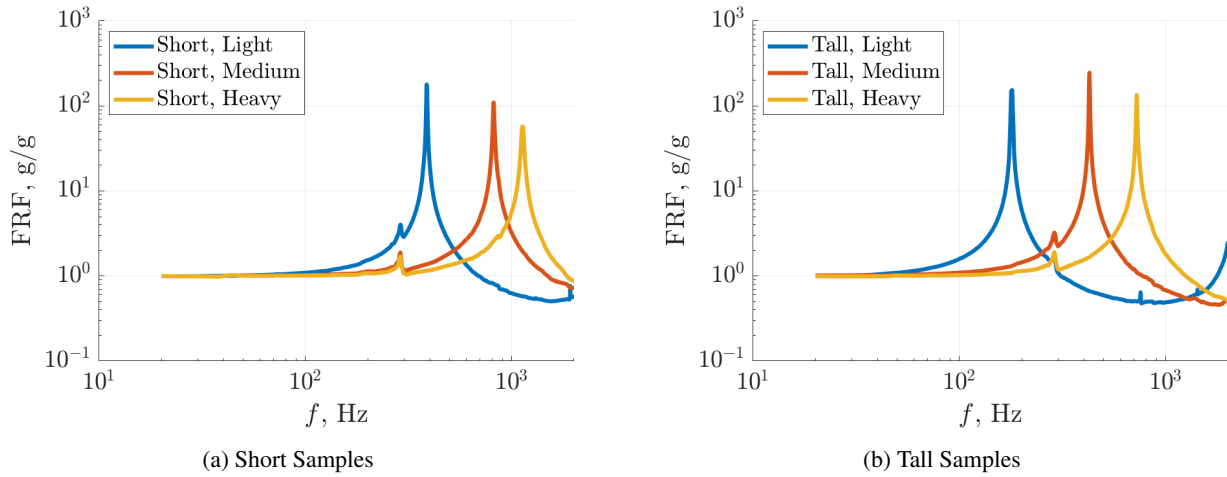


Figure 4: Bending mode - frequency response functions.

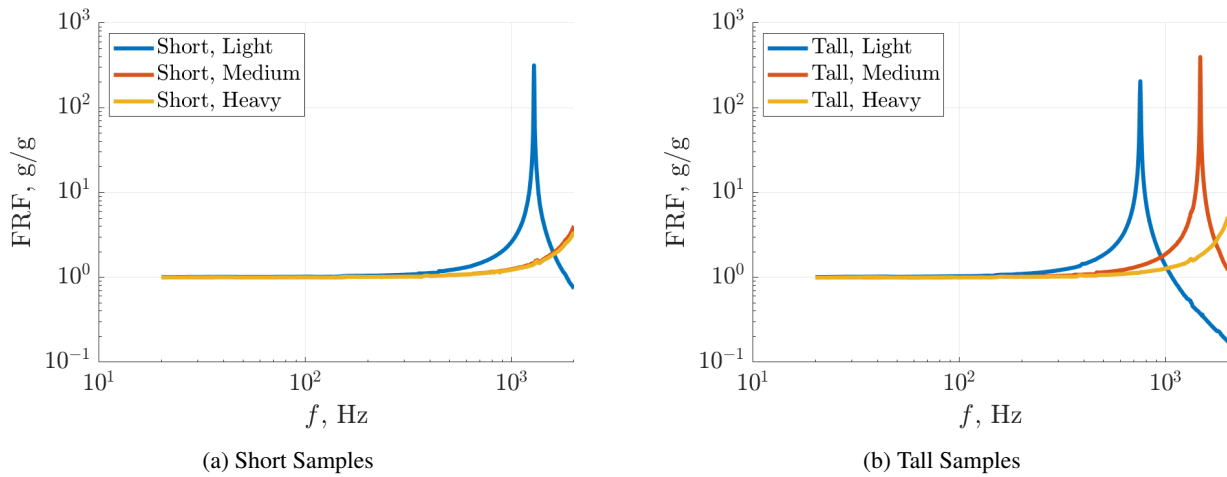


Figure 5: Axial mode - frequency response functions.

The measured peak frequencies are summarised in Table 5. It also contains the simulated peak frequencies from the modal analyses. The FEA results over-predict the peak frequencies of the bending mode by 17 % to 36 %, and of the axial mode by 13 % to 29 %. The over-predictions could be explained by several assumptions in the FEA. For example, a bonded connection between the sandwich sample and dummy mass, as well neglecting the sample's roughness. A relatively high roughness is typical for EBM parts.<sup>10</sup> A previous study by Hernandez-Nava et al.<sup>13</sup> on Ti-6Al-4V lattice structures found that the roughness can contribute to a significant portion of a strut's diameter. As a result, the load-bearing cross-section would locally be reduced, leading to lower stiffness.

Table 5: Measured and Simulated Peak Frequencies

#	Sample	Bending Mode		Axial Mode	
		Experiment	Simulation	Experiment	Simulation
		$f_{\text{Peak}}$ , Hz	$f_{\text{Peak}}$ , Hz	$f_{\text{Peak}}$ , Hz	$f_{\text{Peak}}$ , Hz
1	Short Sample, Light Lattice	386	470	1280	1528
2	Short Sample, Medium Lattice	846	1065	> 2000	> 2000
3	Short Sample, Heavy Lattice	1122	1524	> 2000	> 2000
4	Tall Sample, Light Lattice	180	210	752	847
5	Tall Sample, Medium Lattice	426	554	1468	1892
6	Tall Sample, Heavy Lattice	722	883	> 2000	> 2000

The analytical predictions for the Young's moduli based on the nominal lattice properties are listed in Table 6. The predicted values for the short and the tall samples are virtually identical as the predictions only take relative lattice

## MECHANICAL PROPERTIES OF TITANIUM ALLOY SANDWICH STRUCTURES

density and not the lattice height into account. Naturally, the equivalent Young's modulus increases with growing lattice density. Table 6 also contains the Young's modulus computed from the experimentally measured peak frequencies using the SDOF approximations (Equations 1 and 3). The computed Young's moduli based on the bending mode measurements (using Equation 1) are much lower than the analytical predictions (at least 13 times lower). This indicates that the initial approximation using the cantilever beam model is inadequate for the sample's bending mode since the requirement of a long tall beam is not fulfilled. A more involved analytical model should be employed.

The computed Young's modulus values based on the axial mode measurements are in closer agreement with the analytical predictions (only up to 4 times lower). As mentioned above, the slight over-prediction of the analytical models could also be caused by geometric imperfections (such as surface roughness) of the printed lattice structures. The over-prediction of the Young's modulus using Equation 5 was similarly found by Galati et al.<sup>11</sup> in compression tests of Ti-6Al-4V lattice structures with relative densities  $\approx 20\%$ .

The analytical predictions of the relative Young's modulus  $E_{\text{relative}} = E_{\text{lattice}}/E_{\text{solid}}$  are plotted in Figure 6 including the three available values from the axial load case. The increase of the relative Young's modulus of the short samples seems to correspond to the prediction of Equation (6), although more samples are needed to confirm this result.

Table 6: Young's Moduli from Analytical Predictions Based on Nominal Lattice Properties (Equations 5 and 6), as well as from SDOF Approximations Based on Measured Peak Frequencies (Equations 1 and 3)

#	Sample	Analytical Prediction		SDOF Approximation	
		Foam <sup>12</sup>	BCC <sup>23</sup>	Bending Mode	Axial Mode
		$E_{\text{foam}}$ , GPa	$E_{\text{bcc}}$ , GPa	$E_{\text{lattice}}$ , GPa	$E_{\text{lattice}}$ , GPa
1	Short Sample, Light Lattice	0.28	0.67	0.01	0.29
2	Short Sample, Medium Lattice	1.61	1.70	0.06	-
3	Short Sample, Heavy Lattice	3.60	2.66	0.11	-
4	Tall Sample, Light Lattice	0.28	0.67	0.01	0.17
5	Tall Sample, Medium Lattice	1.64	1.70	0.07	0.64
6	Tall Sample, Heavy Lattice	3.64	2.66	0.20	-

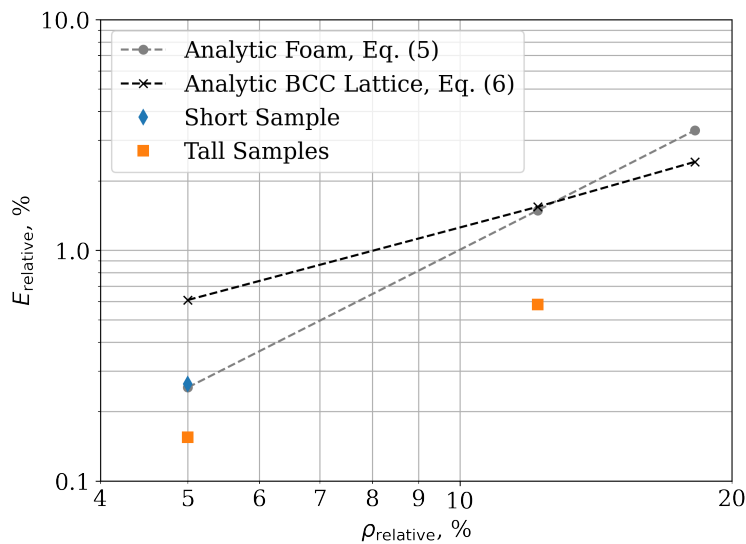


Figure 6: Calculated equivalent Young's moduli using the spring-mass model, as well as analytical predictions of Gibson and Ashby<sup>12</sup> and Zhang.<sup>23</sup>

#### 4. Conclusions

In this study, the equivalent Young's moduli of Ti-6Al-4V sandwich structures with lattice cores were extracted from non-destructive vibration tests. The computed Young's moduli based on the axial load cases using a spring-mass SDOF system seems to be in reasonable agreement with analytical predictions for cellular materials and ranged from 0.17 GPa to at least 0.64 GPa. A cantilever beam SDOF system was found to be an inadequate approximation for the bending

## MECHANICAL PROPERTIES OF TITANIUM ALLOY SANDWICH STRUCTURES

mode of the samples tested. Future work could include the implementation of a more suitable model system for an improved approximation of the lateral load case. Moreover, further testing is planned involving a larger dummy mass to decrease the peak frequencies of the axial mode of all samples below 2000 Hz, and larger acceleration loads.

## 5. Acknowledgments

We would like to acknowledge the Creative Design and Additive Manufacturing Lab at the University of Auckland for their support in designing the samples, as well as Zenith Technica Ltd. for their expertise and swift execution of the sample manufacturing.

## References

- [1] M. Ashby. The properties of foams and lattices. *Philosophical Transactions of the Royal Society A: Mathematical, Physical and Engineering Sciences*, 364(1838):15–30, Jan. 2006.
- [2] M. F. Ashby, A. G. Evans, N. A. Fleck, L. J. Gibson, J. W. Hutchinson, and H. N. G. Wadley. *Metal Foams: A Design Guide*. Elsevier, 2000.
- [3] S. Bouslog. 3D Printing Heat Shields. In *Additive Manufacturing & Advanced Materials Workshop*, Houston, TX, USA, June 2017.
- [4] L.-Y. Chen, S.-X. Liang, Y. Liu, and L.-C. Zhang. Additive manufacturing of metallic lattice structures: Unconstrained design, accurate fabrication, fascinated performances, and challenges. *Materials Science and Engineering: R: Reports*, 146:1–56, Oct. 2021.
- [5] Y. Chen, Y. Tao, B. Xu, S. Ai, and D. Fang. Assessment of thermal-mechanical performance with structural efficiency concept on design of lattice-core thermal protection system. *Applied Thermal Engineering*, 143:200–208, Oct. 2018.
- [6] X. Cheng, K. Wei, R. He, Y. Pei, and D. Fang. The equivalent thermal conductivity of lattice core sandwich structure: A predictive model. *Applied Thermal Engineering*, 93:236–243, Jan. 2016.
- [7] ESA. Testing. In *Space engineering*, ECSS-E-10-03A. ESA Requirements and Standards Division, Noordwijk, The Netherlands, 2002.
- [8] ESA. Thermal design data handbook - Part 16: Thermal Protection System. In *Space engineering*, ECSS-E-HB-31-01 Part 16A. ESA Requirements and Standards Division, Noordwijk, The Netherlands, 2011.
- [9] B. Esser, M. Kuhn, I. Petkov, V. Hannemann, J. Barcena, C. Jimenez, A. Okan, S. Ontac, L. Haynes, S. Gianella, A. Ortona, M. Barbato, L. Ferrari, V. Liedtke, D. Francesconi, M. Portaluppi, H. Tanno, T. Uzay, E. Sa, and V. Pereda. Innovative Thermal Management Concepts for Space Vehicles. In *6th European Conference for Aeronautics and Space Sciences*, Krakow, Poland, June 2015.
- [10] W. E. Frazier. Metal Additive Manufacturing: A Review. *Journal of Materials Engineering and Performance*, 23(6):1917–1928, June 2014.
- [11] M. Galati, A. Saboori, S. Biamino, F. Calignano, M. Lombardi, G. Marchiandi, P. Minetola, P. Fino, and L. Iuliano. Ti-6Al-4V lattice structures produced by EBM: Heat treatment and mechanical properties. *Procedia CIRP*, 88:411–416, 2020.
- [12] L. J. Gibson and M. F. Ashby. *Cellular solids structure and properties*. Cambridge University Press, Cambridge, 2nd edition, 1999.
- [13] E. Hernández-Nava, C. Smith, F. Derguti, S. Tammam-Williams, F. Leonard, P. Withers, I. Todd, and R. Goodall. The effect of defects on the mechanical response of Ti-6Al-4V cubic lattice structures fabricated by electron beam melting. *Acta Materialia*, 108:279–292, Apr. 2016.
- [14] V. T. Le, N. S. Ha, and N. S. Goo. Advanced sandwich structures for thermal protection systems in hypersonic vehicles: A review. *Composites Part B: Engineering*, 226:1–44, Dec. 2021.

## MECHANICAL PROPERTIES OF TITANIUM ALLOY SANDWICH STRUCTURES

- [15] K. Lin, K. Hu, and D. Gu. Metallic integrated thermal protection structures inspired by the Norway spruce stem: Design, numerical simulation and selective laser melting fabrication. *Optics & Laser Technology*, 115:9–19, July 2019.
- [16] J. C. Maxwell. L. On the calculation of the equilibrium and stiffness of frames. *The London, Edinburgh, and Dublin Philosophical Magazine and Journal of Science*, 27(182):294–299, Apr. 1864.
- [17] P. Nieke, T. Schleutker, A. Guelhan, N. J. Rattenbury, and J. E. Cater. Additively Manufactured Titanium Alloy Sandwich Structures for Thermal Protection. In *AIAA SciTech 2023 Forum*, National Harbor, MD & Online, Jan. 2023. American Institute of Aeronautics and Astronautics.
- [18] A. Seharng, A. H. Azman, and S. Abdullah. A review on integration of lightweight gradient lattice structures in additive manufacturing parts. *Advances in Mechanical Engineering*, 12(6):1–21, June 2020.
- [19] A. T. Sidor, E. Venkatapathy, and S. A. Bouslog. NASA Efforts to Explore Additively Manufactured Thermal Protection Systems (AMTPS). In *2nd International Conference on Flight Vehicles, Aerothermodynamics and Re-entry Missions & Engineering (FAR)*, Heilbronn, Germany, June 2022.
- [20] G. Welsch, R. Boyer, and E. W. Collings, editors. *Materials Properties Handbook: Titanium Alloys*. ASM International, Materials Park, OH, 1994.
- [21] J. Wijker. *Mechanical Vibrations in Spacecraft Design*. Springer Berlin Heidelberg, Berlin, Heidelberg, 2004.
- [22] Y. Xu, N. Xu, W. Zhang, and J. Zhu. A multi-layer integrated thermal protection system with C/SiC composite and Ti alloy lattice sandwich. *Composite Structures*, 230:1–9, Dec. 2019.
- [23] X. Zhang, H. Zhou, W. Shi, F. Zeng, H. Zeng, and G. Chen. Vibration Tests of 3D Printed Satellite Structure Made of Lattice Sandwich Panels. *AIAA Journal*, 56(10):4213–4217, Oct. 2018.